Reversible Dynamic Behavior in Catalyst Systems: Oscillations of Structure and Morphology

S. Surnev,[1,*] J. Schoiswohl,[1] G. Kresse,[2] M. G. Ramsey,[1] and F. P. Netzer[1,†]

[1]*Institut für Experimentalphysik, Karl-Franzens-Universität Graz, A-8010 Graz, Austria*

[2]*Institut für Materialphysik, Universität Wien, A-1090 Vienna, Austria*

(Received 6 May 2002; published 20 November 2002)

Exposing vanadium oxide nanoparticles on a Pd(111) surface to reducing conditions is shown to cause a spreading of the oxide over the metal until a reduced oxide phase covers the entire surface. Reoxidation reverses this process and oxide island structures and bare metal patches are reestablished. The physical origin of this wetting-dewetting process is revealed at the atomic level by *in situ* variable-temperature scanning tunneling microscopy and in terms of a surface oxide phase stability diagram, as calculated by density functional theory as a function of the chemical potential of oxygen and the vanadium concentration.

DOI: 10.1103/PhysRevLett.89.246101 PACS numbers: 68.47.Gh, 68.35.Md, 68.37.Ef, 71.15.Mb

The cycling between oxidizing and reducing gas feed conditions is a frequently used industrial practice to activate or regenerate supported metal catalysts, which typically consist of metallic nanoparticles dispersed on an inorganic oxide surface [1]. A heterogeneous supported metal catalyst is, however, a complex dynamic system which may change its catalytic properties under such reaction conditions. A common origin for reactivity changes is the modification of the surface structure and morphology of the metal and/or the oxide component of the supported catalyst. Complex physical and chemical interactions at the interface between the metal particles and the oxide support are generally invoked to be responsible for the morphology changes [2,3], which may affect the activity and selectivity of catalysts by influencing the shape of the active metal particles and their balance of surface crystallographic planes. The changes in the morphology of catalysts are often related to a wetting-dewetting behavior of the oxide over the metal phase or vice versa [4], thus emphasizing the significance of material transport processes under reaction conditions on these heterogeneous surfaces.

An important phenomenon affecting the structure and the catalytic performance of oxide supported metals concerns the encapsulation of metal particles with the support material and the decoration of their surfaces with a (partially reduced) oxide layer. Tauster *et al.* have created the term "strong metal-support interaction" (SMSI) to describe the state of a supported metal catalyst, containing a transition metal-oxide with a variety of possible oxidation states as the support material, which as a result of a high temperature reduction treatment showed a significantly lowered chemisorption capacity, as compared to its normal state, but an enhanced reactivity for some catalytic reactions [5,6]. The origin of the SMSI effect has been the subject of much debate in the past years [7], but there is now converging opinion in favor of the so-called encapsulation model, where the metal particles are covered with a thin layer of oxide in a reduced oxidation state [8]. A key issue of SMSI is the reversibility of this effect—the catalyst in the SMSI state can be converted back to its normal state by an oxidizing treatment. The mechanism of oxide migration and of the wetting-dewetting behavior on supported metal catalyst surfaces is a very complex but challenging materials science problem [6]. To reduce the complexity of the parameter space and to separate physical and chemical processes, thereby increasing the experimental transparency and reproducibility, it is well accepted to adopt a reductionist approach in using a *catalyst model system* [9,10]. Here we have employed an *inverse catalyst model system* to study the effects of oxidation and reduction cycles on the morphology of a heterogeneous metal-oxide surface. The *inverse model catalyst* consists of a metal single crystal surface, which is decorated by atomically ordered oxidic nanostructures [11]. We have fabricated a vanadium oxide-on-Pd(111) inverse catalyst surface in ultrahigh vacuum and have investigated the structural changes of the oxide phase as a result of cycled oxidation-reduction conditions using a variable-temperature scanning tunneling microscope (STM) [12]. Here we report the *direct real-space* observation of morphology and structure oscillations of the oxide phase as a result of alternating exposures to H_2 and O_2 at elevated temperature. The physical origin of the morphology and oxidation state oscillations of the oxide overlayer on the metal surface is analyzed by *ab initio* density functional theory (DFT) calculations in terms of the stability and interfacial structure in the Pd-vanadium oxide phase diagram as a function of the oxygen chemical potential.

Ultrathin vanadium oxide layers on Pd(111) develop a pronounced polymorphic behavior: at a given oxide coverage several different oxide phases can coexist on the Pd surface, which are distinguished by novel interface-stabilized structures which have no corresponding stable bulk counterparts [13]. The STM image of Fig. 1(a) illustrates a V-oxide/Pd(111) inverse catalyst surface containing clean Pd(111) areas, islands of a VO_2 type oxide phase

 © 2002 The American Physical Society

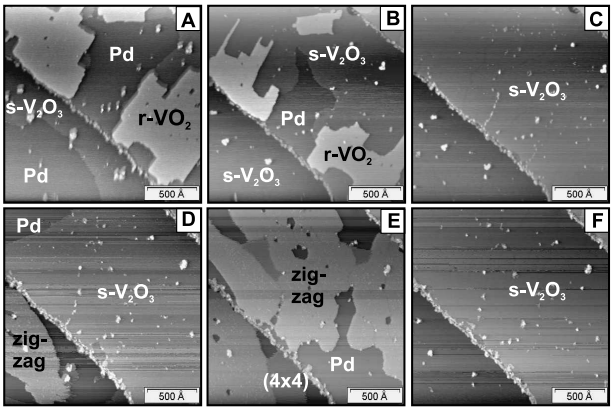

FIG. 1. Sequence of STM images of a vanadium oxide decorated Pd(111) surface exposed to reducing and oxidizing ambient conditions. (a) The Pd(111) surface, annealed at 300 °C in vacuum after oxide deposition, 65% covered with two coexisting V-oxide phases: s-V_2O_3 and r-VO_2. (b) After ~1000 sec exposure to 1×10^{-9} mbar H_2 at 250 °C. (c) After ~2000 sec exposure to 1×10^{-9} mbar H_2 at 250 °C. The surface is now reduced and completely covered by s-V_2O_3. (d) After ~2000 sec exposure of surface (c) to 5×10^{-8} mbar O_2 at 250 °C. The zigzag V_6O_{14} oxide appears. (e) After ~400 sec exposure of surface (d) to 5×10^{-8} mbar O_2 at 250 °C, followed by pump-down of the O_2. The surface contains zigzag V_6O_{14} and (4×4) V_5O_{14} oxide phases along with some free Pd areas. (f) Reduction of surface (e) by ~1250 sec exposure to 3×10^{-9} mbar H_2 at 250 °C. The surface is again wetted by the reduced s-V_2O_3 phase.

with rectangular symmetry (r-VO_2), and a region of a V_2O_3 type oxide phase (s-V_2O_3) with low contrast in the STM image [14]. The atomic-resolution STM images of Figs. 2(a) and 2(b) reveal the atomic structures of these two oxide phases (as shown in the corresponding DFT derived structure models) [13,15]. The interface-stabilized surface-V_2O_3 (s-V_2O_3) phase [Fig. 2(a)] is a true two-dimensional phase with a formal V_2O_3 stoichiometry and consists of a honeycomb vanadium-oxygen arrangement with a (2×2) periodicity with respect to the Pd(111) surface unit mesh; the V atoms are located at the interface to the Pd with the bridging oxygen atoms pointing away from the surface. The rectangular r-VO_2 islands are also only stable in a thin layer limit [16] and are oxygen-terminated on both sides [see structure model 2(b)].

The sequence of STM images Figs. 1(a)–1(c) demonstrates the morphology behavior upon reduction (exposure to 1×10^{-9} mbar H_2 at 250 °C): the r-VO_2 islands shrink in size [Fig. 1(b)] and transform into the s-V_2O_3 phase, which eventually covers the entire surface [Fig. 1(c)]. The reduced s-V_2O_3 oxide thus spreads out and completely wets the Pd surface. This process is reversed by oxidation, the STM images Figs. 1(d)–1(f) were recorded subsequently after Figs. 1(a)–1(c), but in the presence of 5×10^{-8} mbar O_2 at 250 °C. The s-V_2O_3 phase transforms first into the so-called "zigzag vanadium oxide" on oxidation while dewetting the Pd surface [Fig. 1(d)], and then develops into the (4×4) oxide phase; both phases coexist in Fig. 1(e) along with free Pd. The latter two oxide phases correspond to somewhat higher oxidation states of V than in VO_2 and have been rationalized with the help of DFT in terms of V_6O_{14} and V_5O_{14} model structures [see Figs. 2(c) and 2(d)] [17]. Switching back to the hydrogen ambient (3×10^{-9} mbar H_2 at 250 °C) leads to reduction and again to a s-V_2O_3 covered surface [Fig. 1(f)]. These H_2-O_2 cycles can be repeated many times, the oxide displaying the described morphology oscillations between oxidized ($V_{5,6}O_{14}$) and reduced (s-V_2O_3) surface conditions.

The STM observations can be evaluated quantitatively as displayed in Fig. 3, and the analysis has been substantiated by photoelectron spectroscopy (not shown). Figure 3 shows the percentage areas of the bare Pd patches and of the various V-oxide covered parts of the surface during a reduction-oxidation-reduction cycle, plotted versus the time of the experiment. Note that the bare Pd area (solid circles) has disappeared after the first reduction step (~ 2000 sec), the surface being covered entirely by s-V_2O_3, but that after the oxidation step the bare Pd is quantitatively recovered (at ~4750 sec). This indicates that the wetting-dewetting process is completely reversible. The reoxidation of the s-V_2O_3 surface follows a complex pattern as seen in Fig. 3 in the range 2200–5000 sec. After an induction period (2200–4000 sec)

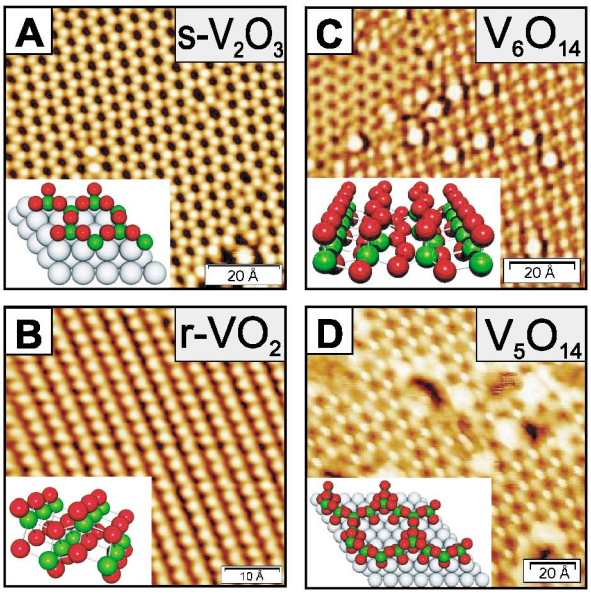

FIG. 2 (color). Atom-resolved STM images of the principal V-oxide "monolayer-type" phases on Pd(111) and corresponding DFT derived structure models. (a) Surface-V_2O_3 phase. (b) Rectangular-VO_2 phase. (c) Zigzag V_6O_{14} phase. (d) (4×4) V_5O_{14} phase. Red spheres: oxygen; green: vanadium; grey: palladium.

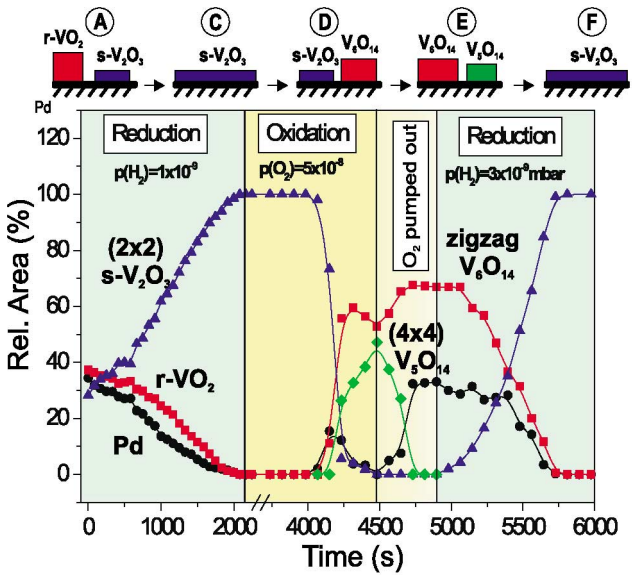

FIG. 3 (color). Percentage areas of bare Pd and various V-oxide covered parts of the surface plotted versus the time during a reduction-oxidation-reduction cycle, as evaluated from STM images. The schematic diagram on top of the figure illustrates the morphology changes, (a)–(f) refer to the STM images of Fig. 1.

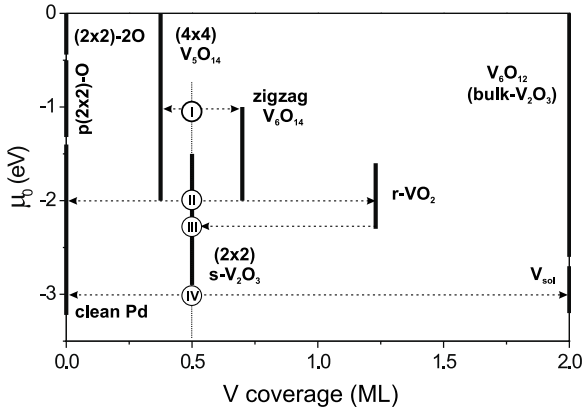

FIG. 4. Phase diagram of V-oxides on Pd(111), as calculated by DFT, as a function of the chemical potential of oxygen μ_O (which is related to the oxygen pressure [19]) and the vanadium coverage. The thick bars indicate the stability regions of the various oxide phases. Points I–IV are discussed in the text; the dotted arrows indicate the coexistence or transformation of oxide phases.

[18], s-V_2O_3 oxidizes first to the zigzag V_6O_{14}, which converts subsequently partially to the (4×4) V_5O_{14} phase; at ~4500 sec both oxides coexist at the surface in approximately equal amounts, a clear result of kinetic effects. At ~4500 sec the gas phase O_2 has been pumped away and the (4×4) oxide transforms back to the zigzag phase under these mildly reducing (vacuum) conditions. At this point the bare Pd area recovers and the surface is partially covered by a single oxide phase (the zigzag V_6O_{14}). Subsequent reduction leads again to the completely wetted, s-V_2O_3 covered surface (5750 sec). This oscillatory morphology cycle, which has been repeated many times, is illustrated schematically in the cartoon at the top of Fig. 3.

The physical origin of the reduction/oxidation behavior of V-oxides on Pd(111) is disclosed in the DFT phase diagram of Fig. 4, where the ranges of stability of the V-oxide phases are indicated by bars in the relevant parameter space of chemical potential of oxygen (μ_O) [19] and V concentration [θ_V, in terms of monolayer (ML) coverages]. For clean Pd(111) ($\theta_V = 0$), chemisorbed oxygen phases [$p(2 \times 2)$-O; (2×2)-2O] are indicated, whereas for $\theta_V \geq 2$ ML, oxygen-terminated bulk-type V_2O_3 (3 layers = V_6O_{12}) represents the stable oxide phase for a wide range of oxygen potentials [13,16]. The range of interest for the "inverse model catalyst" surface concerns $\theta_V \leq 1$ ML. For example, at $\theta_V = 0.5$ ML and $\mu_O = -1.0$ eV (point I), zigzag V_6O_{14} and (4×4) V_5O_{14} coexist at the surface. On lowering the oxygen potential, e.g., to $\mu_O = -2.0$ eV, the $V_{5,6}O_{14}$ oxides are predicted to become unstable and decompose into r-VO_2, s-V_2O_3 and some bare Pd patches (point II in Fig. 4). Under more drastic reduction of μ_O (e.g., ≤ -2.25 eV, point III) the r-VO_2 phase transforms to s-V_2O_3, the s-V_2O_3 phase is thus the only stable V-oxide for low μ_O (in the range -2.25 to -3 eV); it decomposes eventually ($\mu_O \leq -3$ eV, see point IV) and the V atoms dissolve into the Pd bulk (V_{sol}), which is more stable than remaining adsorbed at the Pd surface [16].

The observed sequence of oxide phases upon oxidation-reduction is now readily understood, since oxidizing/reducing experimental conditions lead to an increase/decrease of the chemical potential of oxygen. The surface morphology and the wetting-dewetting behavior is the natural consequence of the spatial lattice arrangement and the packing density of the particular stable oxide phase(s). It is, however, important to recall that the oxide phases in this ultrathin layer limit are (quasi-)two-dimensional materials, which have no corresponding stable bulk structures. Kinetic effects have not been addressed here, but the surface mobility of the oxide species is clearly high, since the migration processes take place readily at 250 °C.

It is useful to add a comment on the traditional framework of describing the wetting-dewetting of an overlayer on a substrate in terms of interfacial energies. For an overlayer to spread out on a substrate (wetting), the interfacial free energies γ must satisfy the relation

$$\gamma_{\text{overlayer}} + \gamma_{\text{interface}} < \gamma_{\text{substrate}},$$

where $\gamma_{\text{overlayer}}$ and $\gamma_{\text{substrate}}$ are the surface free energies of the metal and the oxide overlayer, respectively, and $\gamma_{\text{interface}}$ is the interfacial free energy between substrate and overlayer. The oxides under consideration are the

r-VO_2 and $V_{5,6}O_{14}$ phases under oxidizing conditions, and the s-V_2O_3 and a possible three-dimensional bulk-type V_2O_3 phase under reducing conditions. Since all oxide layers are oxygen-terminated at the outer (vacuum) surface (see Fig. 2 and Ref. [13]), their surface energies may be assumed to be similar to the first approximation. The interfacial free energy $\gamma_{\text{interface}}$ of s-V_2O_3 and bulk-V_2O_3 is then the decisive factor determining the wetting behavior under reducing conditions, and it is essentially determined by the bonding interaction at the oxide-metal interface. The s-V_2O_3 layer is vanadium terminated, but the bulk-V_2O_3 is oxygen terminated at the interface to the Pd [13,16]. The V-Pd bonding is fairly strong and has been calculated by DFT to be $\sim$2.5 eV per V atom, whereas the binding energy between the oxygen-terminated bulk-V_2O_3 and the Pd substrate is much less ($\sim$ 400 meV per O atom). Therefore, $\gamma_{\text{interface}}$ of s-V_2O_3 is much smaller than that of the bulk-type V_2O_3 phase, thus driving the reduced system into a wetting condition.

The inverse catalyst model system employed in this study has allowed the specification at the atomic level of the structures and the energetics of the different oxide phases involved in the observed morphology changes during oxidation-reduction cycles on a heterogeneous metal-oxide surface. It is expected that the observations reported here reflect a more general behavior of wetting-dewetting on heterogeneous transition metal-oxide–metal surfaces, and that quasi-two-dimensional oxide phases specific to the metal-oxide interface play a decisive role in the materials transport processes on supported metal catalysts.

This work was supported by the Austrian Science Foundation.

*Corresponding author.
Electronic address: svetlozar.surnev@uni-graz.at
†Corresponding author.
Electronic address: falko.netzer@uni-graz.at

[1] G. A. Somorjai, *Introduction to Surface Chemistry and Catalysis* (Wiley, New York, 1994).
[2] *Metal-Support Interactions in Catalysis, Sintering, and Redispersion*, edited by S. A. Stevenson, J. A. Dumesic, R. T. K. Baker, and E. Ruckenstein (Van Nostrand Reinhold, New York, 1987).
[3] X. Lai and D. W. Goodman, J. Mol. Catal. A **162**, 33 (2000).
[4] B. S. Clausen *et al.*, Top. Catal. **1**, 367 (1994).
[5] S. J. Tauster, S. C. Fung, R. T. K. Baker, and J. A. Horsley, Science **211**, 1121 (1981).
[6] S. J. Tauster, Acc. Chem. Res. **20**, 389 (1987).
[7] G. L. Haller and D. E. Resasco, Adv. Catal. **36**, 173 (1989).
[8] O. Dulub *et al.*, Phys. Rev. Lett. **84**, 3646 (2000).
[9] G. A. Somorjai and M. X. Yang, J. Mol. Catal. A **115**, 389 (1997).
[10] M. Boudart, Top. Catal. **13**, 147 (2000).
[11] F. P. Leisenberger *et al.*, Surf. Sci. **444**, 211 (2000).
[12] The experiments were carried out in an ultrahigh vacuum variable-temperature STM (Oxford Instruments) at $\sim$250 °C in the presence of O_2 or H_2 ambients, using a tracking software algorithm to compensate for the small thermal drift of the instrument. The same area of the surface could therefore be imaged during the time of the whole experiment (1–2 h).
[13] S. Surnev *et al.*, Phys. Rev. Lett. **87**, 086102 (2001).
[14] The V-oxide decorated Pd(111) surface has been prepared by evaporating 0.5 ML vanadium metal [1 ML is related to the atomic density of the Pd(111) surface, i.e., corresponds to 1.52×10^{15} V atoms/cm^2] in 2×10^{-7} mbar O_2 onto the clean Pd(111) surface at 250 °C, followed by gentle annealing at 300 °C.
[15] S. Surnev *et al.*, Phys. Rev. B **61**, 13 945 (2000).
[16] G. Kresse *et al.*, Surf. Sci. **492**, 329 (2001).
[17] Note that the stoichiometry of the V_5O_{14} model is only formally higher than V_2O_5, since the oxygen termination at the oxide-metal interface is shared with the Pd surface atoms. Both zigzag and (4×4) oxide models are experimentally supported by STM and phonon spectra in high-resolution electron energy loss spectroscopy. The (4×4) and zigzag V-oxides transform into VO_2 and s-V_2O_3 upon annealing in vacuum to $\geq$ 300 °C.
[18] The induction period is presumably due to the necessity of generating sufficient free Pd sites (starting at defects) for the activation (dissociation) of O_2.
[19] The chemical potential μ_O is related to the oxygen pressure p and the temperature through $\mu_O(T, p) = \mu_O(T, p^0) + 1/2kT \ln(p/p^0)$. $\mu_O = 0$ corresponds to a pressure at which oxygen condenses at the surface; $\mu_O = -1$ eV corresponds to $p \approx 10^{-7}$ mbar at 520 K.